Investigations for the Optimization of Metal Freeforming using the ARBURG freeformer

N. Krischke*, M. Friedmann*, and J. Fleischer*

*wbk Institute of Production Science, Karlsruhe Institute of Technology (KIT), Kaiserstr. 12, 76131 Karlsruhe, Germany

Abstract

The ARBURG freeformer represents an additive manufacturing system for producing thermoplastic components using commercially available polymer granulate. This fabrication process offers the potential to use feedstocks known from the metal injection molding (MIM) sector to manufacture so-called green parts. These parts consist of 60 Vol.-% stainless steel powder and 40 Vol-% organic polymer binding system. By debinding and sintering these green parts, it is possible to economically produce full metal components with mechanical properties comparable to metal injection molding. In this publication, the process of producing stainless steel parts with ARBURG plastic freeforming will be presented. The mechanical properties and part density are optimized by varying manufacturing parameters and raw materials. Furthermore, concepts to optimize and increase the service life of the nozzle are shown and discussed. An increase of at least 250% could be achieved by plasma nitriding and coating components of the discharge system.

Introduction

Additive Manufacturing (AM) can be used to produce complex components without tools and with maximum freedom of design, starting from a single batch. From a virtual model, parts are physically built layer-by-layer in an automated process (DIN EN ISO/ASTM 52900). AM technologies to process polymers, metal and ceramics are widely used in research and industry, from early product development to high-volume series production (Bourell 2016). Common metal AM processes are Powder Bed Fusion (PBF), direct energy deposition (DED) and material extrusion (MEX). Among these technologies, material extrusion can work with industrially available, low-cost material coming from the Metal Injection Molding (MIM) industry sector. Its process chain neither involves loose metal powder nor requires expensive and harmful high-power sources. The advantages in safety and cost, as well as the existing expertise in the process chain originating from MIM, made this technology grow in recent years (Suwanpreecha and Manonukul 2022).

The company ARBURG launched the ARBURG freeformer in 2013. This 3D printer can process a wide variety of standard thermoplastic polymer granulate coming from injection molding. An advantage to other systems is its open machine control to adapt nearly all processing parameters to meet different requirements from the material or the user's needs (Neff and Kessling 2014). In 2018, by adapting process parameters, the successful processing of MIM feedstock could be shown (Spiller and Fleischer 2018). In this case, 60 Vol-% carbonyl iron powder and a polymer binder system were used to produce green parts. The green parts needed to be debindered and sintered. This resulted in densification and shrinkage of the final solid parts.

The optimization of Metal Freeforming using ARBURG freeformer has been the subject of recent research. This publication shows the results of processing stainless steel powders and evaluating the resulting parts according to their density and geometrical shrinkage compared to formerly used carbonyl iron.

State of the Art

AM processes based on material extrusion offer freedom of design through their layer-based production. Parts are produced cost and resource-efficient. No additional part-specific tools are required (Gibson et al. 2021). ARBURG plastic freeforming (APF) can be used for rapid prototyping and rapid manufacturing of functional polymer parts. The ARBURG freeformer is set up as depicted in Figure 1. The granulated thermoplastic polymer is fed into a heated plastification cylinder and melted as in the injection molding process. The extrusion screw transports the molten polymer through rotation into the material reservoir at the nozzle. Due to the translatory movement of the screw and a backflow barrier at the screw's tip, a variable pressure is applied to the polymer melt in the reservoir. The nozzle opening is normally closed by a needle. A pulsed piezo actuator lets the needle move up and down to discharge individual droplets with a controllable volume. The stationary discharge unit applies the droplets with a variable frequency of up to 333 Hz layer by layer onto a movable part carrier. Two stacked linear motors move the carrier precisely in X- and Y-direction. A spindle drive moves the platform down by a one-layer thickness after a layer is finished. The workspace can be heated up to 100°C to reduce warping (Gaub 2016).

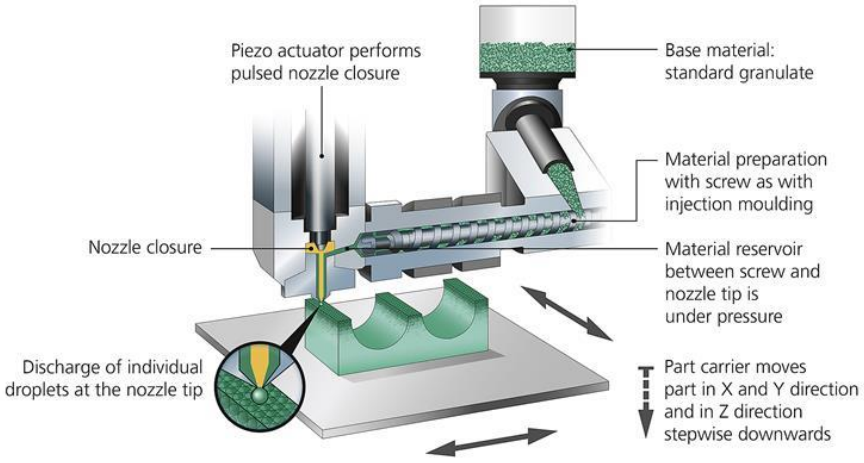

Figure 1: Schematic setup of the functional principle of ARBURG freeformer (Gaub 2016)

For Metal Freeforming, the process chain is comparable to Metal Injection Molding, as shown in Figure 2. The granulate used consists of a fine metal powder. The opening gap at the nozzle tip of the freeformer limits the maximum particle size to less than 12 µm. In the past, the carbonyl iron powder CIP OS from BASF met this criterium (Spiller and Fleischer 2018). Nowadays, through the innovations in powder-bed fusion and microMIM, many more metal alloys and particle size distributions are commercially available (Suwanpreecha and Manonukul 2022). The metal powder is extensively mixed with a thermoplastic binder system and granulated into feedstock. Melting the feedstock and discharging droplets, the freeformer prints green parts layer-by-layer. After the shaping process, green parts need to be debindered. This can be done solvent-based, thermally or catalytic depending on the binder system. In our case, the binder consists of low-density polyethylene (LDPE), paraffin wax and stearic acid. The debinding is done with a hexane bath for up to 24 hours and a subsequent thermal debinding at 600°C under an argon atmosphere. The now so-called brown parts are sintered with a hydrogen atmosphere at 1250°C.

This process chain leads to parts with up to 99.2% of tensile strength R_m compared to MIM (Spiller and Fleischer 2018).

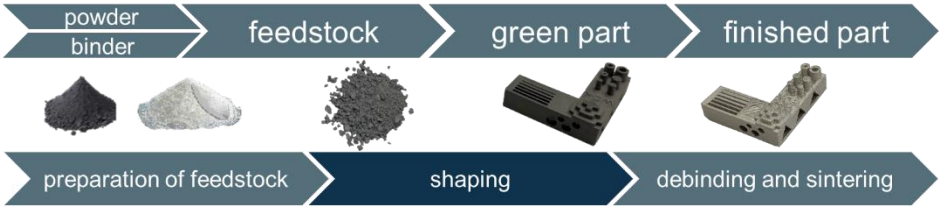

Figure 2: Exemplary MIM process chain

Many process parameters can influence the mechanical and visual properties of printed parts with the ARBURG freeformer. Layer thickness is a standard variable known from other 3D printing processes. It is mainly responsible for the part's surface roughness and building time. A Freeformer-specific variable is the form factor of a droplet. It is defined as the ratio of the width to the height of the droplet, where the height is equivalent to the layer thickness. In addition to the form factor, the discharge number mainly defines the manufacturing process. The discharge number defines the mass output over a specific time. It is coupled to the needle's opening frequency and the carrier's velocity. Keeping the discharge number constant and varying the form factor influences the density of the printed part. Overfilled parts or a regular porosity result from an inadequate initial adjustment of the form factor and discharge number. In Figure 3, the volume of the droplet in form of the discharge number is constant. The droplets are modeled as squares with an edge length of B. While the form factor is reduced, droplets overlap leading to overfilling.

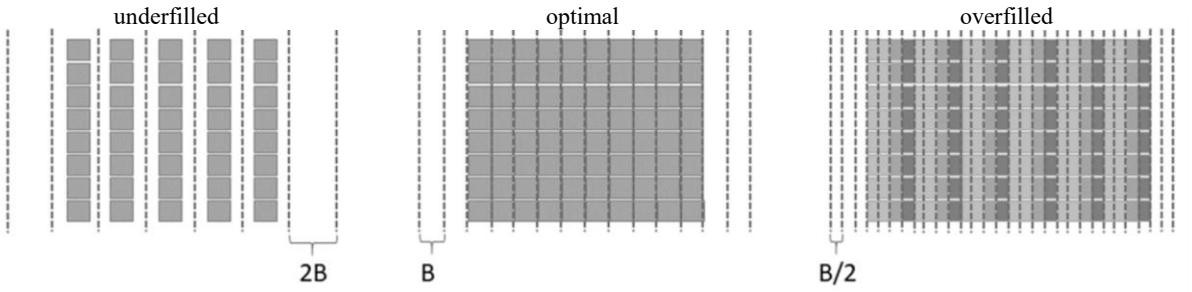

Figure 3: Effect of variable form factor with constant discharge number

In (Spiller 2019), the optimal process parameters for a feedstock with carbonyl iron have been determined. Nevertheless, initial experiments with the former parameter set and newly produced feedstock led to unsatisfying results shown in Figure 4. In addition, carbonyl iron is not a material commonly used for AM. Switching to stainless steel like 316L opens up a lot more possibilities in terms of industrial applications (Gonzalez-Gutierrez et al. 2018). New stainless steel feedstock needs to be characterized and produced. High density and geometric accuracy are achievable by optimizing form factor and discharge number.

Figure 4: Sample cube with the optimal set of parameters from (Spiller 2019)

Experimental Investigation

For the production of new feedstock, the metal powder needs to be characterized to adapt the formula of the binder system to its properties. The original carbonyl iron powder from BASF, as well as two stainless steel 316L powders from Atmix and Sandvik Osprey, meet the strict particle size criterion of a maximum particle diameter less than 12 µm and are hence characterized. The actual particle size distribution, the density and the specific surface area are measured. With these values, the formula of the binder system is adapted accordingly and new feedstock can be produced. It is characterized by the torque profile in a laboratory compounder and its flow properties measured by capillary rheometry. The feedstock is used to print cubic samples that are analyzed by their geometric accuracy. Their density is determined via Archimedes' principle. Based on these results, optimal printing parameters are derived. Wear effects are investigated and possible concepts for an elongation of the service life of the discharge unit are proposed.

Characterization of metal powder

To produce feedstock comparable to (Spiller 2019), the same binder system has been employed. It consists of low-density polyethylene (LDPE) as a backbone combined with paraffin wax and stearic acid as a dispergator. The average density, the specific surface area and the particle size distribution of the metal powder must be known to achieve the optimum mixing ratio of the components. The average density for each metal powder has been measured using a helium pycnometer. The results are listed in Table 1. In addition, the specific surface area provides information about the porosity of the particles and the required amount of dispergator. It has been measured using gas absorption with the BET method. As stated in the previous chapter, the ARBURG Freeformer requires a maximum particle size of less than 12 µm. With the help of a laser diffractometer, the particle size distribution has been analyzed. All three metal powders meet the criterion. Moreover, 90% of the particles are smaller than at least 6.85 µm in the case of the Atmix 316L powder.

Table 1: Measured material properties of metal powder

	BASF CIP OS	Atmix 316L	Osprey 316L
Average density [g/cm³]	7.4881	7.7326	7.8391
Specific Surface Area [m²/g]	0.8328	0.3576	0.4279
Particle size D-90% [µm]	5.8647	6.8521	6.1077

Characterization of feedstock

Badges of 400 grams each have been produced using a heated laboratory kneading compounder that can measure the driving torque of the mixer. After one hour of kneading and a constant temperature of 125°C, a plateau was reached with the minimum torque shown in Table 2. The plateau indicates the equilibrium zone with a constant level of dispersion. As a rule of thumb, a value around 10 Nm promises good processing possibilities (Nötzel and Hanemann 2020). Calculated from the volumetric fractions, the resulting theoretical density is as well shown in Table 2.

Table 2: Measured properties of the metal feedstock

	BASF CIP OS	Atmix 316L	Osprey 316L
Theoretical density [g/cm³]	4.8578	5.0684	5.0045
Minimum torque [Nm]	10.920	7.578	10.745

For a better prediction of the feedstock's flow behavior, high-pressure capillary rheometry is used. This method helps to measure characteristics of the molten feedstock even under high shear rates as found in the discharge unit of the ARBURG Freeformer. Figure 5 shows the viscosity and shear stress as a function of the applied shear rate. All feedstocks show similar shear-thinning behavior. Higher shear rates (>1500 1/s) as in the ARBURG Plastic Freeforming cause a drop in viscosity to around 150 Pa*s.

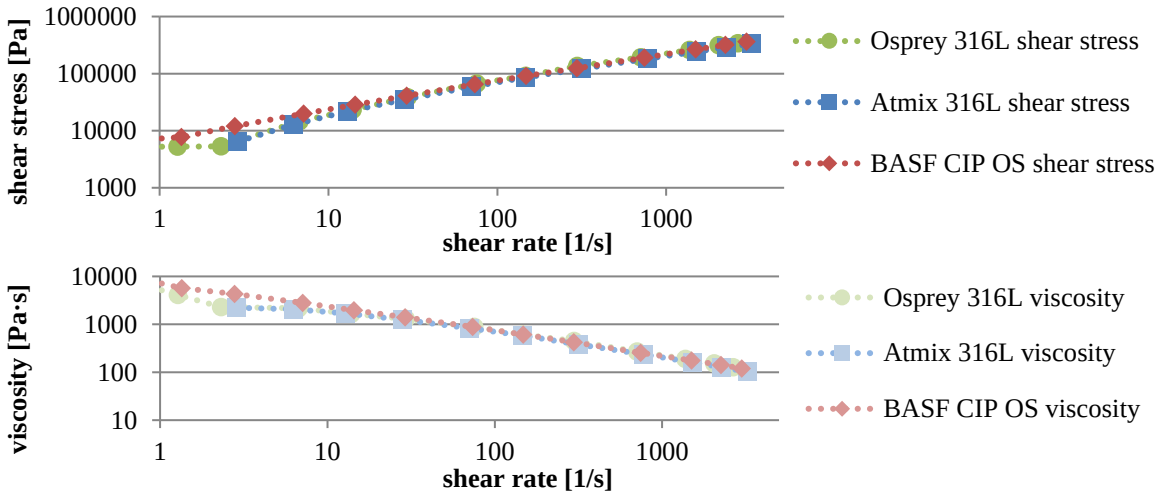

Figure 5: Viscosity and shear stress of metal feedstocks

Characterization of green parts

In the next step, sample cubes with an edge length of 10 mm and a height of 5 mm were printed using the characterized metal feedstocks with the Arburg freeformer. Using the optimum processing temperature of 160°C at the nozzle and 140°C at the material extruder, known from former research by (Spiller and Fleischer 2018) provided good results. Nevertheless, new requirements demand a layer thickness of 0.2 mm, making preliminary studies on a possible process window for discharge number and form factor necessary. With these findings, a partial factorial experimental design can be established to investigate the influence of discharge number and form factor. The final factor levels are shown in Table 3. For each metal feedstock, all five parameter combinations were printed ten times resulting in 150 samples in total.

Table 3: Printing parameters and factor levels of experimental design

discharge number	form factor	layer thickness	temperature
75%	1.3	0.2 mm	160°C - 140°C
75%	1.6	0.2 mm	160°C - 140°C
85%	1.45	0.2 mm	160°C - 140°C
95%	1.3	0.2 mm	160°C - 140°C
95%	1.6	0.2 mm	160°C - 140°C

The samples were printed in randomized batches of 10 with pairs of two of each parameter set to minimize interference with other factors. After processing one of the metal feedstocks, the material extruder and discharge unit were cleaned thoroughly to avoid cross-contamination.

With all cubic samples being printed, measurements for the investigation of geometric accuracy by a micrometer and the average density calculated by Archimedes' principle on a precision scale were carried out. The average height, length and width of each parameter set for all

three materials (BASF CIP OS, Osprey 316L, Atmix 316L) with their standard deviation are shown in Figure 6. Regarding the height, all samples were above 5 mm. The highest deviation can be seen with a discharge number of 95% and a form factor of 1.3. Similar results were acquired for the length and width, whereas the deviation of this parameter set was even higher. Parts printed with a form factor of 1.6 had the lowest values for all three geometric values. Interestingly enough, no clear tendency for one of the three tested feedstocks can be seen. All three provide similar values within the standard deviation.

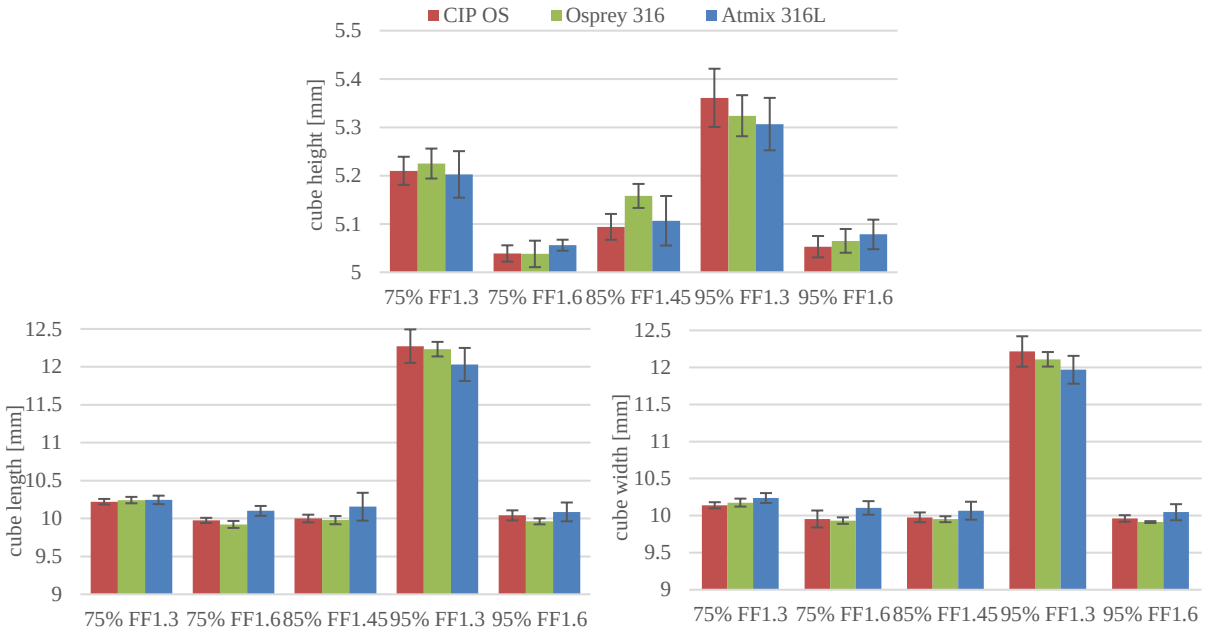

Figure 6: Geometric measurements of the cube samples for different parameter sets

In Figure 7, the left diagram shows the average volume for each parameter set and feedstock. The expected value of 0.5 cm³ could be met by the parameter set of a discharge number of 85% and a form factor of 1.45 and for a discharge number of 95% and a form factor of 1.6. The highest deviation can again be observed for the form factor of 1.3. Regarding the average density shown in the diagram on the right of Figure 7, a clear tendency for the different materials can be seen. This tendency is in line with the theoretical densities of the feedstocks determined earlier, with the Atmix 316L feedstock being the densest and the BASF CIP OS feedstock the least dense. The densities for a form factor of 1.6 are the lowest in comparison. Only the parameter set of 95% discharge number and a form factor of 1.3 comes near the theoretical densities.

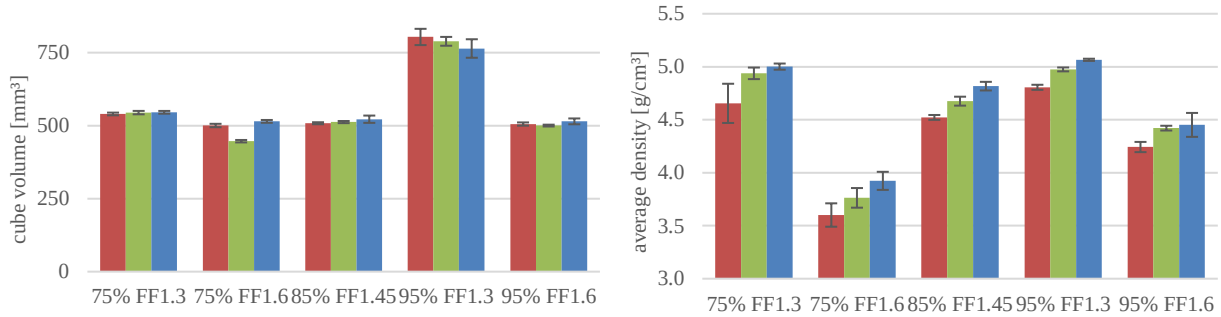

Figure 7: Volume and density of the cube samples for different parameter sets

The high densities measured can be misleading. Both parameter sets with a form factor of 1.3 are overfilled clearly. This can be seen in the geometrical measurements as well as in the optical analysis of the cubic samples. Figure 8 shows an exemplary selection of samples from the Osprey 316L test set. The parameter combinations with a form factor of 1.6 are underfilled. A finding that is also indicated by the density measurement.

Figure 8: Samples with Osprey 316L feedstock

Therefore, the value for the degree of filling is defined. This value indicates the ratio of the total measured volume to the volume of the theoretical geometry. To reduce the error of the tactile measurement method of the sample's side lengths, the volume is calculated using the weighed mass in air and average density. Overfilled parts will have a degree of filling >1, whereas underfilled parts will have a degree of filling <1. The optimum would be around 1 to achieve a geometrical accurate part with the average density of the used feedstock.

$$\text{degree of filling} = \frac{m_{air}/\rho}{V_{theoretical}}$$

To investigate the influence of the discharge number and the form factor on the degree of filling, the main effects diagram compares differences between the means of each factor level. The correlation of the degree of filling on the factors could be confirmed, as shown by the gradient of the straights in Figure 9. With a constant form factor, the degree of filling increases proportionally to the discharge number. On the other hand, the degree of filling decreases with a higher form factor and constant discharge number. The contour diagram on the right represents the degree of filling as a function of the discharge number and the form factor. This makes it possible to determine the optimum discharge number and corresponding form factor for an optimized degree of filling. The lines describe a range with a constant theoretical degree of filling. The shown diagrams represent the results for the Osprey 316L feedstock. All three feedstocks had similar results without any significant deviations.

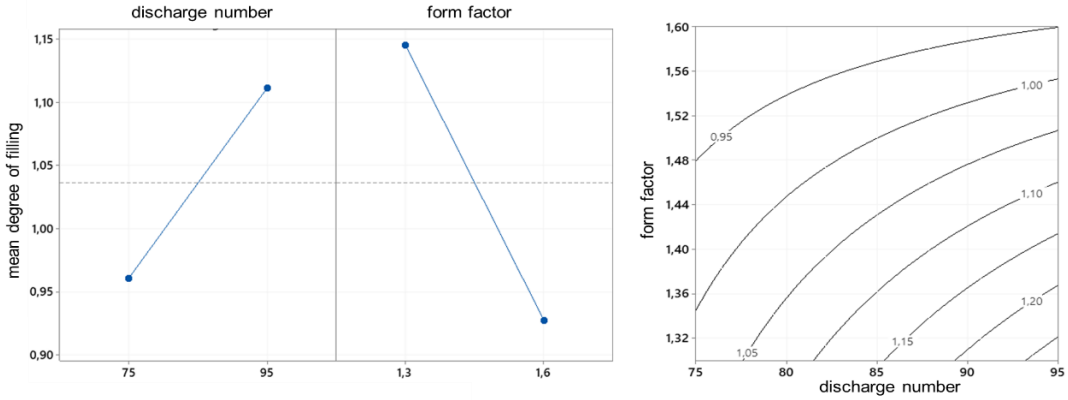

Figure 9: Main effects plot of discharge number and form factor influencing the mean degree of filling (left). Contour diagram with the optimal degree of filling for different parameter sets (right).

Concepts to increase service life

The abrasive properties of the feedstock cause the needle inside the nozzle to deform leading to leakage. Low rates of leakage can be compensated by the control system. Nevertheless, the lifetime of a series standard needle is reduced to 8 million opening cycles. Figure 10 shows the needle used for the experiments. 8 million opening cycles represent service life of about 22 hours printing with a drop frequency of 100 Hz. This value is several orders of magnitude lower than for processing unfilled polymers. The needle shows cold-welded spots on the needle tip's surface. Due to the high shear rates at the dynamically moving needle, the feedstock tends to segregate in this critical area. Uncoated metal particles are now in direct contact with the needle surface. The adhesion of metal particles favors the surface's abrasion over time. Signs of abrasion can be seen in a ring-like form at the needle's tip. The TiCN coating of the needle has been degraded and the raw base material is revealed. Such large deformations cause a leakage rate too high to be compensated and the discharge unit has to be replaced prematurely.

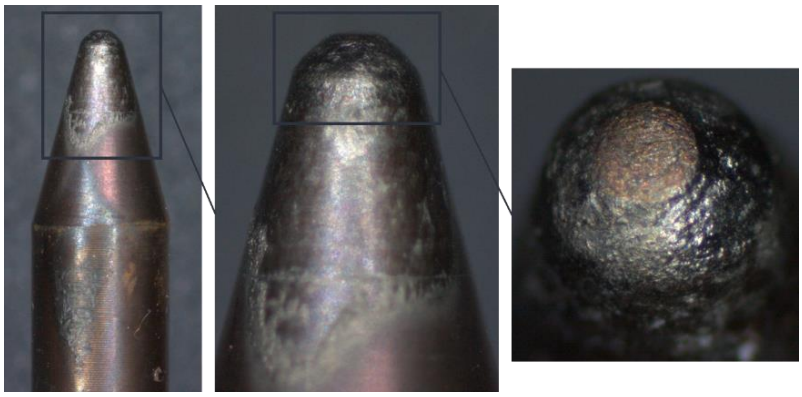

Figure 10: Used series standard needle (TiCN coating) with leakage after 8.8 million cycles working with Osprey 316L feedstock

A possible solution to counteract the adhesion of particles and early abrasion could be the replacement of the needle tip's base material and a hardening coating with a reduced tendency to adhesion. The material replacement for the complete needle is not practicable due to the requirement for a specific spring stiffness. But the exchange of the needle tip is possible using a variety of joining processes. Possible materials could be tungsten cobalt carbides, high-speed steel or bor and silicon nitride as materials nearly as hard as diamond. Exclusively or in combination a coating can be applied. For tools, different titanium carbides and nitrides are available using vapor deposition processes. Higher hardness, lower adhesion tendency and better wear resistance are the main characteristics of these coatings. Tungsten carbides can be applied by thermal spraying. A diamond-like-carbon coating with high-density carbon layers leads to properties comparable to diamond. Needle prototypes applying these techniques have yet to be produced.

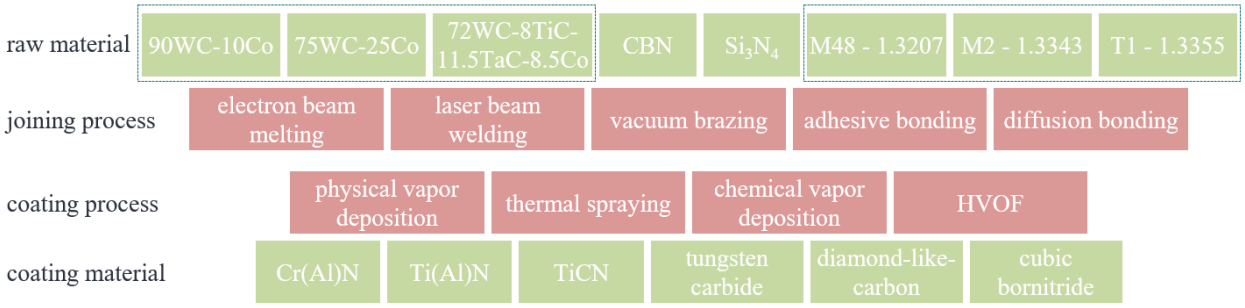

Figure 11: Possible material and coating concepts to elongate the lifetime of the needle

Conclusion

Combining the findings, an optimized parameter set for printing stainless steel 316L feedstock with the ARBURG Freeformer was identified. The main effects plot and the contour diagram show an optimum for the discharge number at around 85%. A matching form factor of 1.5 for this discharge number results in a mean degree of filling of 1.0. Different stainless steel 316L powders compounded with the same binder system provided similar results. From these results, it may be concluded that the main influencing factor in processing is the applied binder system. Future research has to examine the material behavior in terms of shrinkage and porosity after debinding and sintering freeformed parts.

The discharge unit showed above-average wear at the needle tip. To avoid cold-welding of metal particles and the abrasion of the needle surface, the material at the needle's tip must be replaced or hardening coatings applied. In further investigations, the effect on the service life of these concepts must be evaluated.

Acknowledgments

We want to thank ARBURG GmbH + Co. KG for their cooperation and expertise. The production of feedstock was carried out by Steffen Antusch and his team at IAM – Institute of Applied Materials at KIT. This research was funded by the Deutsche Forschungsgemeinschaft (DFG) as part of the research project FL 197/78-1 "Industrielle Ertüchtigung des ARBURG Freiformens zur Herstellung metallischer Bauteile".

References

Bourell, David L. (2016): Perspectives on Additive Manufacturing. In *Annu. Rev. Mater. Res.* 46 (1), pp. 1–18. DOI: 10.1146/annurev-matsci-070115-031606.

DIN EN ISO/ASTM 52900, 2022: DIN EN ISO/ASTM 52900:2022-03, Additive Fertigung-Grundlagen - Terminologie (ISO/ASTM 52900:2021).

Gaub, Heinz (2016): Customization of mass-produced parts by combining injection molding and additive manufacturing with Industry 4.0 technologies. In *Reinforced Plastics* 60 (6), pp. 401–404. DOI: 10.1016/j.repl.2015.09.004.

Gibson, Ian; Rosen, David; Stucker, Brent; Khorasani, Mahyar (2021): Additive Manufacturing Technologies. Cham: Springer International Publishing.

Gonzalez-Gutierrez, Joamin; Cano, Santiago; Schuschnigg, Stephan; Kukla, Christian; Sapkota, Janak; Holzer, Clemens (2018): Additive Manufacturing of Metallic and Ceramic Components by the Material Extrusion of Highly-Filled Polymers: A Review and Future Perspectives. In *Materials (Basel, Switzerland)* 11 (5). DOI: 10.3390/ma11050840.

Neff, Martin; Kessling, O. (2014): Layered Functional Parts on an Industrial Scale. Arburg Plastic Freeforming Permits Additive Manufacturing from Standard Granulate. In *Kunststoffe International* (08/2014), pp. 64–67.

Nötzel, Dorit; Hanemann, Thomas (2020): New Feedstock System for Fused Filament Fabrication of Sintered Alumina Parts. In *Materials (Basel, Switzerland)* 13 (19). DOI: 10.3390/ma13194461.

Spiller, Quirin (2019): Additive Herstellung von Metallbauteilen mit dem ARBURG Kunststoff-Freiformen. [1. Auflage]. Düren: Shaker Verlag (Forschungsberichte aus dem wbk, Institut für Produktionstechnik, Karlsruher Institut für Technologie (KIT), Band 224).

Spiller, Quirin; Fleischer, Jürgen (2018): Additive manufacturing of metal components with the ARBURG plastic freeforming process. In *CIRP Annals* 67 (1), pp. 225–228. DOI: 10.1016/j.cirp.2018.04.104.

Suwanpreecha, Chanun; Manonukul, Anchalee (2022): A Review on Material Extrusion Additive Manufacturing of Metal and How It Compares with Metal Injection Moulding. In *Metals* 12 (3), p. 429. DOI: 10.3390/met12030429.